



**HAL**  
open science

**Hematological disorder associated  
Cxcr4-gain-of-function mutation leads to uncontrolled  
extrafollicular immune response Short title: Cxcr4  
signaling and the extrafollicular response**

Nagham Alouche, Amélie Bonaud, Vincent Rondeau, Rim Hussein-Agha,  
Julie Nguyen, Valeria Bisio, Mélanie Khamyath, Etienne Crickx, Niclas  
Setterblad, Nicolas Dulphy, et al.

► **To cite this version:**

Nagham Alouche, Amélie Bonaud, Vincent Rondeau, Rim Hussein-Agha, Julie Nguyen, et al.. Hematological disorder associated Cxcr4-gain-of-function mutation leads to uncontrolled extrafollicular immune response Short title: Cxcr4 signaling and the extrafollicular response. *Blood*, 2021, 137 (22), pp.3050-3063. 10.1182/blood.2020007450 . hal-03314577

**HAL Id: hal-03314577**

**<https://hal.science/hal-03314577>**

Submitted on 5 Aug 2021

**HAL** is a multi-disciplinary open access archive for the deposit and dissemination of scientific research documents, whether they are published or not. The documents may come from teaching and research institutions in France or abroad, or from public or private research centers.

L'archive ouverte pluridisciplinaire **HAL**, est destinée au dépôt et à la diffusion de documents scientifiques de niveau recherche, publiés ou non, émanant des établissements d'enseignement et de recherche français ou étrangers, des laboratoires publics ou privés.

# **Hematological disorder associated *Cxcr4*-gain-of-function mutation leads to uncontrolled extrafollicular immune response**

Short title: *Cxcr4* signaling and the extrafollicular response

Nagham Alouche<sup>1,2\*</sup>, Amélie Bonaud<sup>1,3,4\*</sup>, Vincent Rondeau<sup>1,3,4</sup>, Rim Hussein-Agha<sup>1</sup>, Julie Nguyen<sup>2</sup>, Valeria Bisio<sup>1,3,4</sup>, Mélanie Khamyath<sup>1,3,4</sup>, Etienne Crickx<sup>5</sup>, Niclas Setterblad<sup>6</sup>, Nicolas Dulphy<sup>1,3,4</sup>, Matthieu Mahevas<sup>5</sup>, David H. McDermott<sup>7</sup>, Philip M. Murphy<sup>7</sup>, Karl Balabanian<sup>1,3,4#</sup>, Marion Espéli<sup>1,3,4#§</sup>

<sup>1</sup> Université de Paris, Institut de Recherche Saint Louis, EMiLy, Inserm U1160, F-75010 Paris, France

<sup>2</sup> Inflammation Chemokines and Immunopathology, Institut National de la Santé et de la Recherche Médicale (INSERM), Faculté de Médecine, Université Paris-Sud, Université Paris-Saclay, Clamart, France

<sup>3</sup> CNRS, GDR3697 "Microenvironment of tumor niches", Micronit, France.

<sup>4</sup> OPALE Carnot Institute, The Organization for Partnerships in Leukemia, Hôpital Saint-Louis, Paris, France.

<sup>5</sup> Institut Necker-Enfants Malades-INSERM U1151/Centre National de la Recherche (CNRS) UMR8633, Université Paris Descartes, Faculté de Médecine, Paris, France.

<sup>6</sup> Institut de Recherche Saint Louis, Paris, France. Université Paris Diderot, Sorbonne Paris Cité, Paris, France

<sup>7</sup> Molecular Signaling Section, Laboratory of Molecular Immunology, National Institute of Allergy and Infectious Diseases, National Institutes of Health, Bethesda, MD, 20892, USA.

\*: co-first authors

#: co-last authors

§ correspondence: Marion Espéli ([marion.espeli@inserm.fr](mailto:marion.espeli@inserm.fr))

Word count: 4338

Abstract word count: 162

Number of figures: 7

Number of references: 47

**Key points:**

- CXCR4 desensitization dampens B cell cycle and differentiation upon TLR activation.
- CXCR4 desensitization limits the strength and length of the extrafollicular immune response.

**Abstract**

The extrafollicular immune response is essential to generate a rapid but transient wave of protective antibodies upon infection. Despite its importance, the molecular mechanisms controlling this first response are poorly understood. Here, we demonstrate that enhanced *Cxcr4* signaling due to defective receptor desensitization leads to exacerbated extrafollicular B cell response. Using a mouse model bearing a gain of function mutation of *Cxcr4* described in two human hematological disorders, WHIM syndrome and Waldenström's Macroglobulinemia, we demonstrated that mutant B cells exhibited enhanced mTOR signaling, cycled more and differentiated more potently into plasma cells than wild-type B cells upon TLR stimulation. Moreover, *Cxcr4* gain-of-function promoted enhanced homing and persistence of immature plasma cells in the bone marrow, a phenomenon recapitulated in WHIM syndrome patient samples. This translated in increased and more sustained production of antibodies upon T-independent immunization in *Cxcr4* mutant mice. Thus, our results establish that fine-tuning of *Cxcr4* signaling is essential to limit the strength and length of the extrafollicular immune response.

## Introduction

Following infections, rapid production of neutralizing antibodies (Abs) through the extrafollicular immune response is essential to control infectious agents. Despite the central importance of this pathway in humoral immunity, the molecular mechanisms at play are poorly understood. Early B cell activation and differentiation initiated through crosslinking of the B cell receptor (BCR) and Toll-like receptors (TLRs) leads to the production of low affinity Abs by short-lived extrafollicular plasma cells (PCs), also called plasmablasts (PBs), which provide rapid but transient protection against infection<sup>1</sup>. Upon T-cell help, this early response can evolve through the formation of germinal centers (GC), to the production of high-affinity long-lived PCs that can persist for an extended period of time in the bone marrow (BM) contributing to immunological memory<sup>2</sup>. The chemokine receptor Cxcr4 and its ligand Cxcl12 are important for the T-dependent immune response through regulation of GC B cell localization and BM homing of PCs<sup>3-8</sup>. However, the role of this axis in early extrafollicular B cell response following antigenic challenge has never been addressed. Upon Cxcl12 binding, Cxcr4 signals through the G proteins. Signal duration and strength is tightly regulated by receptor desensitization which involves phosphorylation of the C-terminal tail of Cxcr4 and the subsequent recruitment of  $\beta$ -arrestins leading to both uncoupling of the receptor from G proteins and receptor internalization<sup>9</sup>. Our group and others have established that this desensitization step is defective in the rare primary immunodeficiency disease WHIM syndrome (WS)<sup>10,11</sup>, which is caused by autosomal dominant mutations in the C-tail of CXCR4, resulting in a gain-of-function in response to CXCL12<sup>10,12</sup>. Strikingly, similar mutations of CXCR4 have been reported in Waldenström's Macroglobulinemia, an indolent lymphoplasmacytic B-cell lymphoma characterized by an IgM spike and BM infiltration of malignant clones with an immunophenotype ranging from activated B cells to PCs<sup>13-15</sup>. *CXCR4* mutations are observed in ~30% of Waldenström's Macroglobulinemia patients in conjunction

with a gain of function mutation of the TLR adaptor *MYD88*<sup>16,17</sup>. Whether and how *CXCR4* and *MYD88* mutations synergize in Waldenström's Macroglobulinemia is still unclear; however, their coincidence in this disease prompted our interest in investigating the general importance of Cxcr4 signaling in the context of TLR-induced MyD88 signaling for B cell and PC biology. Here, using a mouse model<sup>18</sup> bearing an orthologous *Cxcr4* mutation observed both in WS and Waldenström's Macroglobulinemia<sup>13,19</sup>, we demonstrate an unexpected and central role for Cxcr4 desensitization in regulating the early extrafollicular antibody response.

## **Material and Methods**

### **Mice:**

*Cxcr4*<sup>+/*1013*</sup> mice were generated as previously described<sup>18</sup>. *Blimp1*<sup>GFP/+</sup> mice were obtained from Dr. S. Nutt (WEHI, Australia)<sup>20</sup> and crossed with *Cxcr4*<sup>+/*1013*</sup> mice. Mice aged 8-16-week-old or 1-year old and co-housed littermates were used in all experiments that were conducted in compliance with the European Union guide for the care and use of laboratory animals, have been reviewed and approved by an institutional review committee (C2EA-26, Animal Care and Use Committee, Villejuif, France).

### **Human samples:**

Cryopreserved BM aspirates from two WS patients (1 male, 47-year-old, and 1 female >30-year-old at sampling, both bearing the *CXCR4*<sup>R334X</sup> mutation) (collected under NIH protocol 09-I-0200) were provided through a Material Transfer Agreement in accordance with NIH human subject research policies. BM from hip replacement surgery was obtained from discarded material from 6 patients (4 males and 2 females, 42-58 years-old at sampling). All the required ethical and export approvals were obtained from the French Ministries of Health and Agriculture. All individuals provided written informed consent before sampling and data registering. The study was approved by the Comité de Protection des Personnes Ile-de-France VII (Protocol 17-030, n° ID-RCB: 2017-A01019-44). Samples were stained with the antibodies indicated in Supplementary table 1.

### **Immunization:**

Mice were immunized intra-peritoneally with 25 µg of 4-hydroxy-3-nitrophenylacetyl-lipopolysaccharide (NP-LPS) or 25 µg of NP-Ficoll (Biosearch Technologies). Blood, spleen

and BM were harvested and analyzed 3, 6, 12 and 45 days after challenge with NP-LPS and 6 days after NP-Ficoll immunization.

#### **Single cell suspension and flow cytometry:**

Isolation of organs was performed and single cell suspensions were stained as previously described<sup>7</sup>, using the Abs described in Supplementary Table 1. Analyses were carried out on an LSRII Fortessa flow cytometer (BD Biosciences) and data were analyzed with the Flowjo software (TreeStar, Ashland, OR).

#### ***In vitro* functional assays:**

For functional assays, total splenocytes or B cells isolated using a naïve mouse B-cell (CD43<sup>-</sup>) isolation kit (Miltenyi Biotec) were cultured using complete medium (RPMI with 10% fetal calf serum, 1% penicillin/streptomycin, 50  $\mu$ M  $\beta$ -mercaptoethanol, 1 mM sodium pyruvate (All from Gibco)) with 1 U/mL of IL-4 (Miltenyi) and 5 ng/mL of IL-5 (Miltenyi) supplemented with 1  $\mu$ g/mL LPS (Invivogen) or 10  $\mu$ g/mL CpG ODN (Invivogen) and/or 50 nM Cxcl12 (R&D) and/or 10  $\mu$ M AMD3100 (Sigma Aldrich) for 5 minutes and up to 5 days at 37°C. MK-2206 (Ambeed) and Rapamycin (Life Technologies) were used at 1  $\mu$ M and 50 nM respectively. Phosphoflow was performed with the PerFix EXPOSE kit (Beckman Coulter). PB differentiation and apoptosis were assessed by flow cytometry (Supplementary Table 1). For proliferation, splenocytes were loaded with Cell Trace Violet (CTV) (Thermofisher) according to manufacturer's instructions and then stimulated. For cell cycle analysis, cells were permeabilized and fixed with the Foxp3/Transcription Factor Staining Buffer Set (eBioscience) and labeled with an anti-Ki-67 antibody and DAPI was added just before analysis.

#### **Adoptive transfer experiments:**

Splenocytes from WT x Blimp1<sup>GFP/+</sup> and *Cxcr4*<sup>+/-1013</sup> x Blimp1<sup>GFP/+</sup> mice were stimulated *in vitro* with LPS for 4 days. Cells from each genotype were loaded with either CTV or CT Yellow (CTY) (Thermofisher). A 50:50 mix of cells was made and checked by flow cytometry prior to injection. 10<sup>6</sup> cells were transferred intravenously (*i.v.*) into C57Bl/6J CD45.1 WT recipients. Blood, BM and spleens were harvested and analyzed at 24 and 48 hours post transfer.

### **Transwell migration assay:**

Chemotaxis assays were performed using a Transwell assay as previously described<sup>10</sup>. Splenocytes were incubated for 45 minutes at 37°C before migration for 3 hours through a 5 µm pore Transwell insert (Corning) with medium only or with Cxcl12 (R&D) in the lower chamber. Input cells that migrated to the lower chamber were collected, stained and enumerated by flow cytometry. The fraction of cells migrating across the membrane was calculated as follows: [(number of cells migrating to the lower chamber in response to chemokine or medium) / (number of cells added to the upper chamber at the start of the assay)] x 100.

### **Immunofluorescence:**

Spleens were fixed for 4 hours in PBS-paraformaldehyde 4% and incubated overnight in PBS-sucrose 20% before being embedded in OCT (TissueTek). Cryosections were permeabilized with PBS Triton X-100 0.5% for 15 min, washed twice with PBS and blocked with PBS BSA 5%. Sections were stained with primary Abs and secondary Ab (Supplementary table 1) and Hoechst 33342. Slides were scanned using a NanoZoomer Digital Pathology system using X40 objective lenses with numerical aperture 0.75 (Hamamatsu Photonic). BM embedding, sectioning and staining were performed as described<sup>21</sup>. 30 µm sections were permeabilized, saturated and stained as for the spleen. Images were acquired using a TCS SP8 confocal microscope and processed and quantified with Fiji and Imaris.

**ELISA and ELISpot:**

Anti-NP and anti-IgM ELISA were performed as previously described<sup>7</sup>. Enumeration of total IgM and NP-specific IgM ASCs were performed by incubating spleen or BM cells overnight at 37°C on plates pre-coated with NP15-BSA or goat anti-mouse IgM at 5 µg/mL and saturated with culture medium containing 10% FCS. Plates were then washed and incubated with peroxidase-conjugated goat anti-mouse IgM (Southern Biotech). Spots were revealed with AEC (Sigma-Aldrich) and analyzed using an AID ispot Reader (Autoimmun Diagnostika GMBH).

**Time lapse imaging:**

B cells were isolated and stimulated with LPS (see section *in vitro* assays). Cells were either imaged using a Biostation NIKON in a 37°C, 5% CO<sub>2</sub> supplemented chamber at a concentration of 10<sup>4</sup> cells/mL or using the Incucyte® S3 at a concentration of 10<sup>4</sup> cells per well. Cells were imaged for phase-contrast and GFP fluorescence each 15 or 30 minutes, respectively. Images and movies were analyzed with the biostation IM software, the Incucyte S3 software and Fiji.

**Multiplex qPCR**

Multiplex qPCR analysis was performed using the Biomark system (Fluidigm). 75 cells per well were sorted directly into reverse transcription/pre-amplification mix, as previously described<sup>22</sup> (See Supplementary Table 2). Targeted cDNA pre-amplification was performed before processing with Dynamic Array protocol according to the manufacturer's instructions (Fluidigm). Mean expression of *Actb* and *Gapdh* was used for normalization.

**Statistical analysis:**

Data are expressed as means  $\pm$  SEM. The statistical significance between groups was evaluated using the two-tailed unpaired Mann-Whitney non-parametric test (Prism software, GraphPad) unless indicated otherwise in figure legends. Heatmaps were presented using the Z score and clustering analyses were performed using the Pearson rank correlation test (<http://www.heatmapper.ca>). PCA analysis was performed using R ggplot packages.

## Results

### Cxcr4 desensitization limits plasma cell generation

To better understand the pathophysiology of WS, we previously generated a knock-in mouse model bearing a heterozygous nonsense point mutation common to a subset of patients (mutation C1013G in the open reading frame)<sup>18</sup>. These mice, referred to as *Cxcr4*<sup>+/<sup>1013</sup></sup>, phenocopy pan-leukopenia, a major hematological feature of the disease<sup>18</sup>. Moreover, using this model, we recently showed that the gain of function of Cxcr4 affects in a B-cell intrinsic manner the T-dependent humoral immune response recapitulating vaccination failure reported in some WHIM syndrome patients<sup>7,12,23,24</sup>. We took advantage of this model to assess whether Cxcr4 signaling may play a role in the early extrafollicular response and in particular upon stimulation with MyD88-dependent TLR ligands. First, we stimulated *in vitro* splenic B cells from WT and *Cxcr4*<sup>+/<sup>1013</sup></sup> mice with the TLR4 and TLR9 ligands, LPS and CpG respectively, in the presence or absence of Cxcl12. Under these conditions PB differentiation, defined as formation of B220<sup>low</sup>CD138<sup>+</sup> cells, was increased for B cells from *Cxcr4*<sup>+/<sup>1013</sup></sup> mice (Figure 1A-B and Figure S1A-B) and was associated with a 2-fold increase in IgM concentration measured in the culture supernatant (Figure 1B, right panel). The addition of Cxcl12 to the TLR agonists in the stimulation medium led to a small increase of PB in both the WT and the *Cxcr4*<sup>+/<sup>1013</sup></sup> B cell cultures (Figure 1B and Figure S1A-B). Interestingly, stimulation with Cxcl12 alone promoted some PB differentiation of *Cxcr4*<sup>+/<sup>1013</sup></sup> B cells, a phenomenon significantly less marked in WT cultures (Figure 1B and Figure S1B). This Cxcl12-mediated PC differentiation was abolished by addition of the Cxcr4 antagonist AMD3100 confirming that Cxcr4 signaling promoted it (Figure S1B). These observations thus hinted towards a role for Cxcr4 signaling in early B cell activation and differentiation upon stimulation with TLR ligands.

We next determined whether the gain of function of Cxcr4 could affect T-independent B cell immune responses *in vivo*. Immunization with the T-independent type 1 antigen NP-LPS did

not correct the severe B cell lymphopenia observed in the spleens of *Cxcr4*<sup>+/<sup>1013</sup> mice<sup>18</sup> (Figure 1C-D). However, compared to WT mice we observed a significant increase in the frequency of splenic PBs in *Cxcr4*<sup>+/<sup>1013</sup> mice from day 3 through day 6 after immunization (Figure 1E-F). Consistent with this, we detected an increased frequency of IgM<sup>+</sup> Ab-secreting cells (ASCs) by ELISpot in the spleens of *Cxcr4*<sup>+/<sup>1013</sup> mice compared to WT mice (Figure 1G, left panel), and an increased titer of total IgM in the serum of mice bearing the *Cxcr4* gain-of-function mutation (Figure S1C). Moreover, the frequencies of NP-specific IgM<sup>+</sup> ASCs in the spleen were increased at day 6 in *Cxcr4*<sup>+/<sup>1013</sup> mice compared to WT mice (Figure 1G, right panel). Importantly, the T-independent B cell response to NP-LPS immunization was also more sustained in *Cxcr4*<sup>+/<sup>1013</sup> mice compared to WT mice as demonstrated by the still elevated frequency and number of PBs observed at day 6 in the mutant mice (Figure 1F-G). Analysis of the splenic PB population by imaging revealed an increased detection of IgM<sup>+</sup> PBs in sections of *Cxcr4*<sup>+/<sup>1013</sup> spleens compared to WT tissues (Figure 1H-I). Similarly, immunization with the T-independent type 2 NP-Ficoll led to increased splenic PBs and increased total IgM<sup>+</sup> serum titers (Figure 1J-K) in the mutant mice compared to controls. Together, these results show that *Cxcr4* desensitization is an important negative regulator of extrafollicular PB generation in the spleen.</sup></sup></sup></sup></sup></sup>

### ***Cxcr4* desensitization limits the entry of B cells into cycle**

We next addressed the cellular mechanism underlying enhanced PB generation in *Cxcr4*<sup>+/<sup>1013</sup> mice. We cultured WT x Blimp1-GFP and *Cxcr4*<sup>+/<sup>1013</sup> x Blimp1-GFP splenic B cells with LPS and assessed the kinetics of appearance of GFP as a readout for PB differentiation by video microscopy. As shown in Figure 2A, some GFP<sup>+</sup> cells were detectable in *Cxcr4*<sup>+/<sup>1013</sup> cultures as early as 46 hours post stimulation while they started appearing in WT cultures 20 hours later (Figure 2A-B). As B cell and PB survival seemed unaffected (Figure S2A-B), this accelerated</sup></sup></sup>

appearance and accumulation of PBs in culture could be due to an enhanced cycling and/or proliferation of B cells and PBs. B cell proliferation, measured by CTV dye dilution *in vitro* after LPS stimulation, was indeed altered in the mutant condition at day 2 both with and without exogenous Cxcl12 addition (Figure 2C-D, Figure S2C). However, from day 3, B cell proliferation was equivalent between WT and mutant B cells (Figure 2D), suggesting this was only a transient phenotype. Likewise, proliferation in newly generated PBs was not different between WT and mutant conditions at any of the time points analyzed (Figure 2E-F and Figure S2D). Previous reports have suggested that B cell differentiation into PB necessitates at least 3 rounds of cell division<sup>25</sup>. Together with our results, this brought us to consider whether it was not the proliferation of B cells *per se* that was affected, but rather their entry into cell cycle. Indeed, we observed a significant increase in the percentage of B cells in cycle, especially in the G1 phase, in *Cxcr4*<sup>+/<sup>1013</sup></sup> cultures compared to WT ones (Figure 2G-H). Addition of Cxcl12 to LPS in the culture medium led to a similar result and treatment with AMD3100 had no effect on the exacerbated entry into cell cycle observed in mutant B cells (Figure S2E-F). As expected, most PBs were cycling<sup>26</sup> and no difference was observed between our two experimental groups for this cell type (Figure 2I). This demonstrates that *Cxcr4* desensitization is an essential negative regulator of B cell entry into cycle and that deregulation of this process contributes to exacerbated PB differentiation.

### **Exacerbated mTORC1 signaling in *Cxcr4*<sup>+/<sup>1013</sup></sup> mutant B cells**

A wealth of literature reports that upon TLR crosslinking B cell activation and proliferation are dependent on PI3K activation and downstream Akt and mTOR signaling<sup>27-30</sup>. Moreover, several works including ours showed that crosslinking of mutant *Cxcr4* on B cells promoted aberrant activation of the Akt and mTORC1 pathways<sup>7,31,32</sup>. We confirmed *ex vivo* that the gain of function of *Cxcr4* led to an exacerbated Akt phosphorylation upon Cxcl12 stimulation in

presence or in absence of TLR crosslinking. However, inhibition of Akt did not impact B cell cycle entry in this system (Figures 2H and S3C). In parallel, we observed that Cxcl12 stimulation led to a transient increase of the mTORC1 target pS6 in B cells while LPS stimulation promoted strong and sustained S6 activation. Importantly, pS6 signaling was significantly increased in mutant B cells compared to WT controls in all conditions and that was even more marked when both Cxcl12 and LPS were used conjointly (Figure 3A-B). Moreover, AMD3100 pre-incubation was reducing the frequency of pS6<sup>+</sup> mutant B cells upon Cxcl12 stimulation hence supporting the role of Cxcr4 gain of function in this process (Figure 3B left panel). These results suggest that the mutant Cxcr4 and TLR4 synergize to promote exacerbated and sustained mTORC1 signaling in *Cxcr4<sup>+1013</sup>* B cells. Furthermore, treatment with the mTORC1 inhibitor Rapamycin significantly reduced LPS-induced cell cycle entry in WT and *Cxcr4<sup>+1013</sup>* B cells (Figure 3C). In line with this, upon Rapamycin treatment mutant B cell differentiation was down to the level observed for untreated WT B cells (Figure 3D). Hence, our data suggest that mutant Cxcr4 and TLR4 signaling synergize to promote stronger mTORC1 signaling leading to increased B cell entry into cycle and subsequently enhanced PB differentiation.

### **Fine-tuning of Cxcr4 signaling regulates plasmablast settling within the bone marrow**

The T-independent extrafollicular B cell response mainly leads to the generation of short-lived PBs, although it has been reported that some may be able to home to and persist in the BM<sup>33-35</sup>. We therefore investigated whether the enhanced extrafollicular response observed in the spleen in *Cxcr4<sup>+1013</sup>* mice was mirrored by changes in BM homing. After NP-LPS immunization, we observed an increased detection of total IgM<sup>+</sup> ASCs from day 3 and of NP-specific IgM<sup>+</sup> ASCs from day 6 in the BM of *Blimp1<sup>+GFP</sup>xCxcr4<sup>+1013</sup>* mice compared to WT mice (Figure 4A-D). This was associated with a five-fold increase in PBs (*Blimp1-GFP<sup>hi</sup>*

CD138<sup>+</sup>) in the BM of mutant mice compared to WT mice from day 3 post-immunization (Figure 4E). Moreover, fully differentiated PCs (Blimp1-GFP<sup>low</sup> CD138<sup>+</sup>) were significantly increased from day 6 in the BM of the *Cxcr4*<sup>+/*1013*</sup> mice compared to their WT littermates (Figure 4E). Consistently, we enumerated *in situ* significantly more IgM<sup>+</sup> PB/PCs *per* mm<sup>2</sup> at day 6 after NP-LPS immunization in the BM sections of *Cxcr4*<sup>+/*1013*</sup> mice compared to WT mice (Figure 4F-G). Thus, *Cxcr4* desensitization is essential to limit BM accumulation of PBs generated through the extrafollicular response.

### **Plasmablasts spontaneously accumulate in the bone marrow in absence of *Cxcr4* desensitization in mouse and human**

Previous reports have suggested that PB/PCs increase with age in mice<sup>36</sup>. Accordingly, one-year-old middle-aged *Cxcr4*<sup>+/*1013*</sup> mice display a very significant increase in the frequency and number of PBs compared to WT mice at steady state that was particularly marked for BM PBs (Figure 5A-D). Thus, the spontaneous and on-going immune response observed in mice as they age appears exacerbated by the *Cxcr4* gain-of-function mutation and this translates into an accumulation of aberrant PBs within the BM.

We next investigated whether *CXCR4* gain-of-function mutations might also distort the basal distribution of PCs in BM from WS patients. To this end, we compared BM samples from two WS patients carrying the heterozygous *CXCR4*<sup>R334X</sup> mutation with aged-matched control BMs. When we compared WS and control BMs, we observed that the frequencies of PBs (CD19<sup>+</sup>CD138<sup>-</sup>) were significantly increased in patients compared to control BM (Figure 5E-F) with the two less mature fractions representing most of the BM PB/PCs in the patient samples (Figure 5G). Altogether, these results suggest that gain of function mutations of *CXCR4* can be associated with spontaneous aberrant accumulation of PBs within the BM in middle-aged mouse and human.

### **Cxcr4 desensitization intrinsically regulates splenic plasmablast homing properties**

We then explored whether the exacerbated PB accumulation within the BM observed in absence of Cxcr4 desensitization could be accounted for by a cell-intrinsic advantage in terms of BM homing. Mutant splenic PBs express slightly but significantly more surface Cxcr4 than their WT counterpart (Figure 6A-B). Moreover, in a transwell-based migration assay mutant splenic PBs migrated more towards Cxcl12 *in vitro* than their WT counterparts and this was abrogated by the addition of AMD3100 (Figure 6C). Moreover, by co-transfer experiments of *in vitro* generated PBs loaded with either CTV or CTY and mixed at a 1:1 ratio (Figure 6D-E) we showed that *Cxcr4*<sup>+/*1013*</sup> mutant PBs had an intrinsic advantage for homing to the BM compared to WT PBs at all time points considered (Figure 6F, left panel) while the reverse was true for the spleen (Figure 6F, right panel). This experiment demonstrates that, on top of their enhanced generation in secondary lymphoid organs, mutant PBs also have an intrinsic advantage in terms of BM homing.

Transcriptional profiling of WT and *Cxcr4*<sup>+/*1013*</sup> BM PBs revealed significant differences with a notable alteration in the expression of several genes involved in cell adhesion and migration (Figure 6G). We thus further assessed the impact of Cxcr4 signaling on the migratory and adhesion properties of BM PBs and PCs. We showed that mutant PBs and PCs had a unique transcriptional profile characterized by increased expression of *Cxcr4*, *Cxcr3*, *Itgal*, *Cd44* and *Itgb1* and decreased expression of *Ccr7*, *Cxcr5*, *Sell* and *Klf2* compared to WT PBs and PCs (Figure 6H). These differences were sufficient to differentially cluster WT and *Cxcr4*<sup>+/*1013*</sup> BM PB/PCs in a principal component analysis (Figure 6I). Moreover, these altered expression were confirmed by classical RT-qPCR (Figure S4A-C) and flow cytometry (Figure 6J and S4D-E). In summary, our data support that Cxcr4 desensitization is a key control mechanism that

intrinsically limits the homing of PBs to the BM and that once there, this gain of function may confer them with specific localization and/or cell-cell interaction potential.

### **Cxcr4 desensitization is essential to limit plasmablast maturation and persistence within the bone marrow**

We last questioned the fate of these aberrant PBs within the BM. The number of PBs in the BM of *Cxcr4*<sup>+/*1013*</sup> mice peaked at day 6, then rapidly declined and was back to the baseline WT level 12 days after NP-LPS immunization (Figure 7A, left panel). In parallel, the number of more mature B220<sup>-</sup> PCs progressively and markedly increased in the BM of *Cxcr4*<sup>+/*1013*</sup> mice, reaching a peak between 8 and 12 days after immunization, and then slowly declined (Figure 7A, right panel). The distinct kinetics for PBs and PCs suggest that PBs reaching the BM of *Cxcr4*<sup>+/*1013*</sup> mice may be able to differentiate into PCs. We exploited our transfer experiments (Figure 6D) and observed that at day 1 in the BM, most of the transferred cells were found in the PB gate (CD138<sup>hi</sup>B220<sup>+</sup>) and very few were detected within the PC gate (CD138<sup>hi</sup>B220<sup>-</sup>) (Figure 7B). At day 2, however, most of the transferred cells were detected amongst the CD138<sup>hi</sup>B220<sup>-</sup> PCs (Figure 7B) and around 80% of them came from the *Cxcr4*<sup>+/*1013*</sup> cells while the reverse was true for PBs (Figure 7C). In addition, we analyzed the expression of key developmental factors of PCs and observed that *Cxcr4*<sup>+/*1013*</sup> BM PBs had a transcriptional profile corresponding to more mature cells than their WT counterparts, albeit less mature than fully differentiated PCs, and characterized by decreased expression of the B cell transcription factors *Pax5* and *Bach2* and enhanced expression of the PC transcription factors *Prdm1*, *Xbp1* and *Irf4* (Figure 7D). Finally, we observed that total and NP-specific IgM<sup>+</sup> ASCs were increased in the BM of *Cxcr4*<sup>+/*1013*</sup> mice compared to the WT ones and this increase was still observed 45 days after immunization (Figure 7E). Thus, *Cxcr4*<sup>+/*1013*</sup> PBs may differentiate into PCs and

persist for over a month in the BM. Altogether our results demonstrate that Cxcr4 desensitization limits both PB maturation into PCs and their persistence within the BM.

## Discussion

Despite its essential role in host protection, how the extrafollicular immune response is regulated remains mysterious. Here we demonstrate that *Cxcr4* desensitization is an essential regulatory mechanism controlling the duration and the strength of Ab production following induction of a T-independent immune response by finely modulating the pool of extrafollicular-derived PCs.

Our data support a critical role for *Cxcr4* desensitization during this process at multiple checkpoints of B cell activation and PC differentiation. First, we observed that impaired *Cxcr4* desensitization led to increased TLR-driven B cell differentiation into PB with as consequences more PBs generated and increased IgM production in the course of an extrafollicular response. This is associated with enhanced entry into cycle and is consistent with previous studies that have linked B-cell division to their capacity to differentiate into PCs<sup>25,37,38</sup>. In addition, we showed that *Cxcr4* gain of function upon *Cxcl12* stimulation and in synergy with TLR signaling promoted induction of the mTORC1 pathways that drive cell cycle entry and PB differentiation. Second, PBs and PCs bearing the *Cxcr4* gain-of-function mutation display an enhanced BM tropism that may not only be due to the gain of function of *Cxcr4 per se* as the expression of a whole range of migration/adhesion factors are modified in PBs in *Cxcr4*<sup>+/<sup>1013</sup> mice including integrins that can be activated by *Cxcr4* signaling<sup>39,40</sup>.</sup>

Third, differentiation of PBs into PCs and their persistence are enhanced in the BM of *Cxcr4*<sup>+/<sup>1013</sup> mice compared to WT mice. This could be due to direct effects of the enhanced *Cxcr4* signaling on the PC maturation transcriptional program. Alternatively or conjointly, different environmental cues specific to mutant PB/PCs and linked with their altered adhesion/migration potential might contribute to this phenomenon. Importantly, some insights gained from the study of a *Cxcr4* gain-of-function mouse model were validated in the BM of WS patients in whom we observed an over-representation of PBs.</sup>

Conceptually our results suggest an important role for *Cxcr4* signaling in limiting both the number of PBs generated but also the laps of time during which Abs generated in the course of a TLR-dependent extrafollicular response are produced. Indeed, *Cxcr4* desensitization not only regulates the early generation of PBs in secondary lymphoid organs after immunization but also their homing to and maturation within the BM, hence ensuring that only a few PCs generated during this response persist in the BM. As such, *Cxcr4* desensitization seems to act as a gatekeeper ensuring that the Abs produced by PBs during the extrafollicular response are restricted to a transient wave of protection. Limiting PB homing to the BM in this way may also avert the filling of BM niches normally dedicated to other cell types, including GC-derived high affinity PCs that start arising around day 9 after immunization<sup>2</sup>. Thus, our results, taken together with our previously published data<sup>7</sup>, suggest that defective long-term vaccine protection, previously reported in WS patients<sup>12,23,24</sup>, may be the consequence of defective PC homeostasis with an over-representation of low affinity extrafollicular PBs and reduced contribution to the humoral response of GC-derived high affinity PCs.

Somatic *CXCR4* mutations are observed in ~30% of Waldenström's Macroglobulinemia patients, most of the time in conjunction with a gain of function mutation of the TLR adaptor *MYD88*<sup>16,17,41,42</sup> and the presence of the two mutations is associated with shorter time to treatment and earlier progression with ibrutinib<sup>13,15,32,43</sup>. Our data thus support that *CXCR4* nonsense mutations leading to premature stop codon may promote BM homing of malignant cells and niche-mediated therapy resistance previously reported in this disease<sup>44,45</sup>. Moreover, they suggest the paradigm-shifting hypothesis of a potential *CXCR4*-dependent extrafollicular origin for Waldenström's Macroglobulinemia malignant clones. Whether *CXCR4* frameshift mutations, also observed in some Waldenström's Macroglobulinemia patients, may have similar impact remains to be evaluated<sup>46,47</sup>.

## **Acknowledgements**

We thank M-L. Aknin, Dr. H. Gary, F. Gaudin, V. Nicolas, B. Lecomte (IPSIT, technical facilities PLAIMMO, PHIC, MIPSIT and AnimEx, Clamart), J. Megret, C. Cordier (Flow cytometry core facility, SFR Necker, Paris, France), Dr. P. Chappert, A. Vandenberghe (INEM, Paris, France), C. Doliger and Dr. S. Duchez (flow cytometry core facility IUH Institute, Paris, France) for their technical assistance. We are grateful to Dr. MA. Linterman and Prs. S. Luther and S. Peebles for their comments on our manuscript. The study was supported by the Laboratory of Excellence in Research on Medication and Innovative Therapeutics (LabEx LERMIT) (ME and KB), an ANR JCJC grant (ANR-19-CE15-0019-01), an ANR @RAction grant (ANR-14-ACHN-0008), a Fondation Arthritis grant and a “Fondation ARC pour la recherche sur le cancer” grant (PJA20181208173) to ME, an ANR PRC grant (ANR-17-CE14-0019), an INCa grant (PRT-K 2017) and the Association Saint Louis pour la Recherche sur les Leucémies to KB. D.H.M and P.M.M. are supported by the Division of Intramural Research of the National Institute of Allergy and Infectious Diseases, National Institutes of Health. NA and MK were supported by a PhD fellowship from the French Ministry for education and by a 4<sup>th</sup> year PhD fellowship from the “Fondation ARC pour la recherche sur le cancer” for NA. VR was supported by a PhD fellowship from the FRM and a 4<sup>th</sup> year PhD fellowship from the Ligue Nationale Contre le Cancer. RAH was supported by a master fellowship from the “Fondation ARC pour la recherche sur le cancer”. The "EMiLy" U1160 INSERM unit is a member of the OPALE Carnot institute, The Organization for Partnerships in Leukemia (Institut Carnot OPALE, Institut de Recherche Saint-Louis, Hôpital Saint-Louis, Paris, France. Web : [www.opale.org](http://www.opale.org). Email : [contact@opale.org](mailto:contact@opale.org)).

## **Author contribution**

NA designed and performed experiments, analyzed data and wrote the manuscript. AB performed experiments, analyzed data and wrote the manuscript. VR and RHA performed experiments and analyzed data. JN, VB, MK, EC, NS, ND and MM helped with experiments. PMM and DHM provided essential human reagents and reviewed the manuscript. KB contributed to the project design and to the manuscript redaction. ME designed the project, analyzed data and wrote the manuscript.

### **Conflict of Interest**

The authors declare that no conflict of interest exists.

## References

1. MacLennan ICM, Toellner K-MM, Cunningham AF, et al. Extrafollicular antibody responses. *Immunol Rev.* 2003;194(1):8-18. doi:10.1034/j.1600-065X.2003.00058.x
2. Weisel FJ, Zuccarino-Catania G V., Chikina M, Shlomchik MJ. A Temporal Switch in the Germinal Center Determines Differential Output of Memory B and Plasma Cells. *Immunity.* 2016;44(1):116-130. doi:10.1016/j.immuni.2015.12.004
3. Bannard O, Horton RM, Allen CDC, An J, Nagasawa T, Cyster JG. Germinal center centroblasts transition to a centrocyte phenotype according to a timed program and depend on the dark zone for effective selection. *Immunity.* 2013;39(5):912-924. doi:10.1016/j.immuni.2013.08.038
4. Allen CDC, Ansel KM, Low C, et al. Germinal center dark and light zone organization is mediated by CXCR4 and CXCR5. *Nat Immunol.* 2004;5(9):943-952. doi:10.1038/ni1100
5. Hargreaves DC, Hyman PL, Lu TT, et al. A coordinated change in chemokine responsiveness guides plasma cell movements. *J Exp Med.* 2001;194(1):45-56. doi:10.1084/jem.194.1.45
6. Nie Y, Waite J, Brewer F, Sunshine M-J, Littman DR, Zou Y-R. The Role of CXCR4 in Maintaining Peripheral B Cell Compartments and Humoral Immunity. *J Exp Med.* 2004;200(9):1145-1156. doi:10.1084/jem.20041185
7. Biajoux V, Natt J, Freitas C, et al. Efficient Plasma Cell Differentiation and Trafficking Require Cxcr4 Desensitization. *Cell Rep.* 2016;17(1):193-205. doi:10.1016/j.celrep.2016.08.068
8. Victora GD, Schwickert TA, Fooksman DR, et al. Germinal center dynamics revealed by multiphoton microscopy with a photoactivatable fluorescent reporter. *Cell.* 2010;143(4):592-605. doi:10.1016/j.cell.2010.10.032
9. Moore CAC, Milano SK, Benovic JL. Regulation of Receptor Trafficking by GRKs and Arrestins. *Annu Rev Physiol.* 2007;69(1):451-482. doi:10.1146/annurev.physiol.69.022405.154712
10. Balabanian K, Lagane B, Pablos JL, et al. WHIM syndromes with different genetic anomalies are accounted for by impaired CXCR4 desensitization to CXCL12. 2005. doi:10.1182/blood-2004
11. Kawai T, Choi U, Whiting-Theobald NL, et al. *Enhanced Function with Decreased Internalization of Carboxy-Terminus Truncated CXCR4 Responsible for WHIM Syndrome.* Vol 33.; 2005. [https://ac-els-cdn-com.gate2.inist.fr/S0301472X05000378/1-s2.0-S0301472X05000378-main.pdf?\\_tid=1b0dc71b-a9c6-4bd1-ab42-c14136a98417&acdnat=1533984065\\_ef2cb69afb9900f6cf6043c0ab771c7a](https://ac-els-cdn-com.gate2.inist.fr/S0301472X05000378/1-s2.0-S0301472X05000378-main.pdf?_tid=1b0dc71b-a9c6-4bd1-ab42-c14136a98417&acdnat=1533984065_ef2cb69afb9900f6cf6043c0ab771c7a). Accessed August 11, 2018.
12. Gulino AV, Moratto D, Sozzani S, et al. Altered leukocyte response to CXCL12 in patients with warts hypogammaglobulinemia, infections, myelokathexis (WHIM) syndrome. *Blood.* 2004;104(2):444-452. doi:10.1182/blood-2003-10-3532
13. Treon SP, Cao Y, Xu L, Yang G, Liu X, Hunter ZR. Somatic mutations in MYD88 and CXCR4 are determinants of clinical presentation and overall survival in Waldenström macroglobulinemia. *Blood.* 2014;123(18):2791-2796. doi:10.1182/blood-2014-01-550905
14. Poulain S, Roumier C, Venet-Caillaud A, et al. Genomic landscape of CXCR4 mutations in Waldenström macroglobulinemia. *Clin Cancer Res.* 2016;22(6):1480-1488. doi:10.1158/1078-0432.CCR-15-0646
15. Gustine JN, Xu L, Tsakmaklis N, et al. CXCR4 S338X clonality is an important determinant of ibrutinib outcomes in patients with Waldenström Waldenström

- macroglobulinemia. 2019. doi:10.1182/bloodadvances.2019000635
16. Treon SP, Xu L, Hunter Z. MYD88 Mutations and Response to Ibrutinib in Waldenström's Macroglobulinemia. *N Engl J Med.* 2015;373(6):584-586. doi:10.1056/NEJMc1506192
  17. Leblond V, Kastritis E, Advani R, et al. Treatment recommendations from the Eighth International Workshop on Waldenström's Macroglobulinemia. *Blood.* 2016;128(10):1321-1328. doi:10.1182/blood-2016-04-711234
  18. Balabanian K, Brotin E, Biajoux V, et al. Proper desensitization of CXCR4 is required for lymphocyte development and peripheral compartmentalization in mice. 2012. doi:10.1182/blood-2012
  19. Poulain S, Roumier C, Venet-Caillault A, et al. Genomic Landscape of CXCR4 Mutations in Waldenström Macroglobulinemia. *Clin Cancer Res.* 2016;22(6):1480-1488. doi:10.1158/1078-0432.CCR-15-0646
  20. Kallies A, Hasbold J, Tarlinton DM, et al. Plasma Cell Ontogeny Defined by Quantitative Changes in Blimp-1 Expression. *J Exp Med J Exp Med.* 2004;200(8):967-977. doi:10.1084/jem.20040973
  21. Kusumbe AP, Ramasamy SK, Starsichova A, Adams RH. Sample preparation for high-resolution 3D confocal imaging of mouse skeletal tissue. *Nat Protoc.* 2015;10(12):1904-1914. doi:10.1038/nprot.2015.125
  22. Thai LH, Le Gallou S, Robbins A, et al. BAFF and CD4+ T cells are major survival factors for long-lived splenic plasma cells in a B-cell-depletion context. *Blood.* 2018;131(14):1545-1555. doi:10.1182/blood-2017-06-789578
  23. Handisurya A, Schellenbacher C, Reininger B, et al. A quadrivalent HPV vaccine induces humoral and cellular immune responses in WHIM immunodeficiency syndrome. *Vaccine.* 2010;28(30):4837-4841. doi:10.1016/j.vaccine.2010.04.057
  24. Mc Guire PJ, Cunningham-Rundles C, Ochs H, Diaz GA. Oligoclonality, impaired class switch and B-cell memory responses in WHIM syndrome. *Clin Immunol.* 2010;135(3):412-421. doi:10.1016/j.clim.2010.02.006
  25. Hasbold J, Corcoran LM, Tarlinton DM, Tangye SG, Hodgkin PD. Evidence from the generation of immunoglobulin G-secreting cells that stochastic mechanisms regulate lymphocyte differentiation. *Nat Immunol.* 2004. doi:10.1038/ni1016
  26. Fairfax KA, Kallies A, Nutt SL, Tarlinton DM. Plasma cell development: From B-cell subsets to long-term survival niches. *Semin Immunol.* 2008;20(1):49-58. doi:10.1016/j.smim.2007.12.002
  27. Wicker LS, Boltz RC, Matt V, Nichols EA, Peterson LB, Sigal NH. Suppression of B cell activation by cyclosporin A, FK506 and rapamycin. *Eur J Immunol.* 1990;20(10):2277-2283. doi:10.1002/eji.1830201017
  28. Donahue AC, Fruman DA. Proliferation and Survival of Activated B Cells Requires Sustained Antigen Receptor Engagement and Phosphoinositide 3-Kinase Activation. *J Immunol.* 2003;170(12):5851-5860. doi:10.4049/jimmunol.170.12.5851
  29. Yusuf I, Zhu X, Kharas MG, Chen J, Fruman DA. Optimal B-cell proliferation requires phosphoinositide 3-kinase-dependent inactivation of FOXO transcription factors. *Blood.* 2004;104(3):784-787. doi:10.1182/blood-2003-09-3071
  30. Kay JE, Kromwel L, Doe SE, Denyer M. Inhibition of T and B lymphocyte proliferation by rapamycin. *Immunology.* 1991;72(4):544-549. <http://www.ncbi.nlm.nih.gov/pubmed/1709916> <http://www.pubmedcentral.nih.gov/articlerender.fcgi?artid=PMC1384375>.
  31. Roselli G, Martini E, Lougaris V, Badolato R, Viola A, Kallikourdis M. CXCL12 mediates aberrant costimulation of B lymphocytes in warts, hypogammaglobulinemia, infections, myelokathexis immunodeficiency. *Front Immunol.* 2017;8(SEP).

- doi:10.3389/fimmu.2017.01068
32. Roccaro AM, Sacco A, Jimenez C, et al. C1013G/CXCR4 acts as a driver mutation of tumor progression and modulator of drug resistance in lymphoplasmacytic lymphoma. 2014. doi:10.1182/blood-2014-03-564583
  33. Bortnick A, Chernova I, Quinn WJ, Mugnier M, Cancro MP, Allman D. Long-Lived Bone Marrow Plasma Cells Are Induced Early in Response to T Cell-Independent or T Cell-Dependent Antigens. *J Immunol.* 2012;188(11):5389-5396. doi:10.4049/jimmunol.1102808
  34. Taillardet M, Haffar G, Mondière P, et al. The thymus-independent immunity conferred by a pneumococcal polysaccharide is mediated by long-lived plasma cells. *Blood.* 2009;114(20):4432-4440. doi:10.1182/blood-2009-01-200014
  35. Foote JB, Mahmoud TI, Vale AM, Kearney JF. Long-Term Maintenance of Polysaccharide-Specific Antibodies by IgM-Secreting Cells. *J Immunol.* 2012;188(1):57-67. doi:10.4049/jimmunol.1100783
  36. Han S, Yang K, Ozen Z, et al. Enhanced differentiation of splenic plasma cells but diminished long-lived high-affinity bone marrow plasma cells in aged mice. *J Immunol.* 2003;170(3):1267-1273. doi:10.4049/jimmunol.170.3.1267
  37. Tangye SG, Hodgkin PD. Divide and conquer: The importance of cell division in regulating B-cell responses. *Immunology.* 2004;112(4):509-520. doi:10.1111/j.1365-2567.2004.01950.x
  38. Barwick BG, Scharer CD, Bally APR, Boss JM. Plasma cell differentiation is coupled to division-dependent DNA hypomethylation and gene regulation. *Nat Immunol.* 2016;17(10):1216-1225. doi:10.1038/ni.3519
  39. Glodek AM, Honczarenko M, Le Y, Campbell JJ, Silberstein LE. Sustained activation of cell adhesion is a differentially regulated process in B lymphopoiesis. *J Exp Med.* 2003;197(4):461-473. doi:10.1084/jem.20021477
  40. Petty JM, Lenox CC, Weiss DJ, Poynter ME, Suratt BT. Crosstalk between CXCR4/Stromal Derived Factor-1 and VLA-4/VCAM-1 Pathways Regulates Neutrophil Retention in the Bone Marrow. *J Immunol.* 2009;182(1):604-612. doi:10.4049/jimmunol.182.1.604
  41. Hunter ZR, Xu L, Tsakmaklis N, et al. Insights into the genomic landscape of MYD88 wild-Type Waldenström macroglobulinemia. *Blood Adv.* 2018;2(21):2937-2946. doi:10.1182/bloodadvances.2018022962
  42. Cao X xin, Meng Q, Cai H, et al. Detection of MYD88 L265P and WHIM-like CXCR4 mutation in patients with IgM monoclonal gammopathy related disease. *Ann Hematol.* 2017;96(6):971-976. doi:10.1007/s00277-017-2968-z
  43. Cao Y, Hunter ZR, Liu X, et al. The WHIM-like CXCR4 S338X somatic mutation activates AKT and ERK, and promotes resistance to ibrutinib and other agents used in the treatment of Waldenstrom's Macroglobulinemia. *Leukemia.* 2015;29(1):169-176. doi:10.1038/leu.2014.187
  44. Jalali S, Ansell SM. Bone marrow microenvironment in Waldenstrom's Macroglobulinemia. *Best Pract Res Clin Haematol.* 2016;29(2):148-155. doi:10.1016/j.beha.2016.08.016
  45. Ghobrial IM, Maiso P, Azab A, et al. The bone marrow microenvironment in Waldenstrom macroglobulinemia. *Ther Adv Hematol.* 2011;2(4):267-272. doi:10.1177/2040620711410096
  46. Castillo JJ, Xu L, Gustine JN, et al. CXCR4 mutation subtypes impact response and survival outcomes in patients with Waldenström macroglobulinaemia treated with ibrutinib. *Br J Haematol.* 2019;187(3):356-363. doi:10.1111/bjh.16088
  47. Hunter ZR, Xu L, Yang G, et al. The genomic landscape of Waldenström

macroglobulinemia is characterized by highly recurring MYD88 and WHIM-like CXCR4 mutations, and small somatic deletions associated with B-cell lymphomagenesis. *Blood*. 2014;123(11):1637-1646. doi:10.1182/blood

## Figure legends:

**Figure 1: Cxcr4 desensitization limits plasma cell differentiation *in vitro* and *in vivo*:** (A-B) Splenic B cells were cultured in presence of LPS, LPS+Cxcl12, or Cxcl12 alone for 4 days. (A) Representative dot plots for the gating of PBs (B220<sup>lo</sup>CD138<sup>+</sup>) generated *in vitro* after 4 days of culture. (B) The proportion of PBs was determined by FACS (left panel). IgM concentrations in the supernatants were determined by ELISA (right panel). (C) Schematic diagram for the NP-LPS immunization. (D) Frequency of splenic B cells (CD19<sup>+</sup> B220<sup>+</sup>) during NP-LPS immunization. (E) Representative dot plots for PB gating in the spleen of both WT and *Cxcr4*<sup>+/-1013</sup> mice 6 days post NP-LPS immunization. (F) Percentage and total number of PBs in the spleen at day 0, 3 and 6 post immunization. (G) Quantification of total IgM<sup>+</sup> and NP15-specific IgM<sup>+</sup> ASCs in the spleen by ELISpot at day 0, 3 and 6 post immunization. (H) Representative staining of spleen sections from WT and *Cxcr4*<sup>+/-1013</sup> mice at day 3 post immunization. PBs are stained with an anti-IgM Ab (red), basal membrane is stained with an anti-laminin Ab (green) and nuclei are stained with Hoechst 33342 (Blue), Scale bar: 800µm. (I) Quantification of IgM<sup>+</sup> PB accumulation within the spleen at day 3 and 6. (J) Frequency of total PBs and of IgM<sup>+</sup> ASCs determined by flow cytometry and ELISpot, respectively in the spleen 6 days post NP-Ficoll immunization (K) Serum titers of total IgM<sup>+</sup> from both genotypes were measured by ELISA at day 0 and 6 post NP-Ficoll immunization. Results are from 3 independent experiments (A-G and J-K) or one representative experiment out of 2 (H-I) (Mean ± SEM, n=2-7). Mann–Whitney U test was used to assess statistical significance except for (I) where student t-test was used (\*P<0.05, \*\* P<0.01, \*\*\*P<0.001).

**Figure 2: Cxcr4 desensitization limits the entry of B cells into cycle:** (A) Representative fields from time-lapse imaging of splenic B cells from Blimp1<sup>GFP/+</sup> x WT and Blimp1<sup>GFP/+</sup> x *Cxcr4*<sup>+/-1013</sup> mice cultured in the presence of LPS. Images were taken using the Biostation at 46

and 67h post stimulation. Scale bar: 20 $\mu$ m **(B)** Quantification of GFP<sup>+</sup> cells/ imaged fields during LPS stimulation of splenic B cells. GFP fluorescence detection was measured up to 90 hours post stimulation using the Incucyte technology. **(C-F)** Splenocytes from WT and *Cxcr4*<sup>+/*1013*</sup> mice were loaded with CTV and cultured in presence of LPS for 3 days. **(C)** Representative histograms for CTV dilution in LPS stimulated B cells at day 2. **(D)** Frequency of B cells present in each CTV-dilution generation at day 2 and 3. **(E)** Representative dot plots for CTV dilution during PB (CD138<sup>+</sup>) differentiation at day 2 post LPS stimulation. **(F)** Frequency of PBs present in each CTV-dilution generation at day 2 and 3. **(G)** Representative plots showing the different phases of the cell cycle (G0, G1, S, G2-M) for splenic B cells at day 2 post LPS stimulation stained with DAPI and for Ki-67. **(H-I)** Frequency of splenic B cells and PBs in each cell cycle phase at day 2 post LPS stimulation. Results are from 2 independent experiments (C-I) or one representative experiment out of 2 (A-B) (Mean  $\pm$  SEM, n=2-7 for C-H; n=2 for A-B). Mann–Whitney U test was used to assess statistical significance (\*P<0.05, \*\*P<0.01, \*\*\*P<0.001).

**Figure 3: Exacerbated mTORC1 signaling in *Cxcr4*<sup>+/*1013*</sup> mutant B cells:** **(A)** Representative histograms for pS6 in splenic B cells non-stimulated (NS) or stimulated for 5 minutes with Cxcl12, LPS or a combination of both. The impact of Rapamycin on LPS+ Cxcl12 stimulated cells is also shown. **(B)** Quantification of the frequency of pS6<sup>+</sup> B cells among splenocytes non-stimulated, stimulated for 5 minutes or 24 hours with Cxcl12, LPS or a combination of both in presence or in absence of AMD3100. **(C)** Frequency of splenic B cells in each cell cycle phase at day 2 post LPS stimulation in presence or in absence of Rapamycin. **(D)** Frequency of PBs determined by FACS 3 days after LPS stimulation in presence or in absence of Rapamycin. Results are from one representative experiment out of 2-3 **(A-C)** or 2 pooled experiments **(D)** (Mean  $\pm$  SEM, n=4 for A-C; n=6-18 for D). Mann–Whitney U test was used to assess statistical

significance (WT vs *Cxcr4*<sup>+/*1013*</sup>: \*P<0.05, \*\* P<0.01; untreated vs AMD3100: #P<0.05 (Panel 3B); LPS alone vs LPS+Rapamycin: #P<0.05, ### P<0.01(Panels 3C and D)).

**Figure 4: Fine-tuning of *Cxcr4* signaling is required to limit plasmablast accumulation within the bone marrow:** (A) Schematic diagram describing the immunization protocol. Blimp1-GFP expression was used to distinguish PBs (Blimp1-GFP<sup>low</sup> CD138<sup>+</sup>) from PCs (Blimp1-GFP<sup>hi</sup> CD138<sup>+</sup>). (B) Total BM cellularity of both WT and *Cxcr4*<sup>+/*1013*</sup> mice during NP-LPS immunization. (C-D) Quantification and representative spots for total IgM<sup>+</sup> ASCs (C) and NP-specific IgM<sup>+</sup> ASCs (D) in the BM determined by ELISpot at day 0, 3 and 6 post immunization. (E) Representative dot plots for PCs and PBs in the BM of both WT and *Cxcr4*<sup>+/*1013*</sup> mice at day 6 post immunization (left panels). Total cell numbers for BM PBs and PCs at day 0, 3 and 6 are shown (right panels). (F) Representative images of IgM<sup>+</sup> PB/PC staining in BM sections (femur) from WT and *Cxcr4*<sup>+/*1013*</sup> mice at day 6 post immunization. Whole BM imaging is shown only for *Cxcr4*<sup>+/*1013*</sup> mice. Sections were stained with Ab against laminin (green), IgM (red) and nuclei were counterstained with Hoechst 33342 (Grey). Scale bare: 50  $\mu$ m. (G) Quantification of the number of IgM<sup>+</sup> PB/PC per mm<sup>2</sup> fields at day 0 and day 6 post immunization. Results are from 2-4 independent experiments (Mean  $\pm$  SEM, n=5-9 (A-E) or n=3 (G)). Mann-Whitney U test was used to assess statistical significance (\*P<0.05, \*\* P<0.01).

**Figure 5: Plasmablasts spontaneously accumulate in the bone marrow in absence of *Cxcr4* desensitization in mouse and human:** (A) Representative dot plots showing the gating strategy for PBs in the spleen of young and middle-aged (M.A) mice of both genotypes. (B) Frequency and total number of PBs in the spleen of young and M.A. mice (left and central panel). The ratio M.A./young is also represented (right panel). (C) Representative dot plots for

PBs (B220<sup>lo</sup> CD138<sup>+</sup>) and PCs (B220<sup>-</sup> CD138<sup>+</sup>) in the BM of young and M.A. mice from both genotypes. **(D)** Frequency and total number of PBs and PCs in the BM of young and M.A. mice from both genotypes. The ratio M.A./young is also represented (right panel). Results are from 2 independent experiments (Mean  $\pm$  SEM, n=3-12). Mann-Whitney U test was used to assess statistical significance (\*P<0.05, \*\* P<0.01, \*\*\* P<0.001, \*\*\*\*P<0.0001). **(E)** Representative dot plots for the gating strategy of the different PB/PC subsets in the BM of control healthy donor (HD) and WS patients. Mononuclear cells were gated on FSC-A/SSC-A, doublets and dead cells were excluded. On the live cells, T cells were excluded (left panels) and total PB/PC were gated as CD27<sup>hi</sup>CD38<sup>hi</sup> (central panels). The three PB/PC subsets were gated based on the expression of CD19 and CD138 from the less to the more mature: CD19<sup>+</sup>CD138<sup>-</sup> (green box), CD19<sup>+</sup>CD138<sup>+</sup> (blue box) and CD19<sup>-</sup>CD138<sup>+</sup> (red box) (right panels). **(F)** Flow cytometry-based quantification of the frequency of the three subsets among total PCs for control and WS BM. **(G)** Pie chart representation of the contribution of each PB/PC subset to the total BM pool for the control and WS samples. The average contribution of the 3 subsets to the total PC pool for control and WS BM is shown. n=6 for the control BM and n=2 for the WS BM. Unpaired t-test was used to assess statistical significance (\*\* P<0.01).

**Figure 6: Cxcr4 desensitization intrinsically regulates splenic plasmablast homing properties:** **(A)** Representative FACS plot for Cxcr4 surface expression on splenic PBs. The dashed vertical line is placed at the peak of the Cxcr4 staining on WT PBs. **(B)** Quantification of the geometrical mean of Cxcr4 at the surface of splenic PBs (MFI: geometrical mean fluorescence intensity). **(C)** Migration index of splenic PBs to Cxcl12 determined by transwell-based assay. Cxcl12 was added to the lower well at the indicated concentrations with or without AMD3100. **(D)** Schematic diagram describing the transfer experiment protocol. Blimp1<sup>GFP/+</sup> PBs were generated *in vitro* from splenic B cells and labelled with CTV for *Cxcr4*<sup>+/<sup>1013</sup> cells</sup>

and with CTY for WT cells. Labelled WT and mutant cells were mixed at a 1:1 ratio and transferred into CD45.1 WT recipients. **(E)** Representative dot plot of the cell mix (1:1) prior transfer. **(F)** Dot plots showing the percentages of CTV<sup>+</sup> (*Cxcr4*<sup>+/*1013*</sup> x Blimp1<sup>GFP/+</sup>) and CTY<sup>+</sup> (WT x Blimp1<sup>GFP/+</sup>) cells in the BM and the spleen of recipient mice at day 1 post transfer (left panels). Frequency of CTV<sup>+</sup> (*Cxcr4*<sup>+/*1013*</sup> x Blimp1<sup>GFP/+</sup>) and CTY<sup>+</sup> (WT x Blimp1<sup>GFP/+</sup>) cells in the BM and the spleen of recipient mice at day 1 and 2 post transfer (right panels). **(G)** Heatmap showing the relative expression of 60 transcripts from sorted BM PBs from both WT and *Cxcr4*<sup>+/*1013*</sup> mice determined by Biomark multiplex qPCRs at day 6 post immunization with NP-LPS. Data are presented by applying a column Z score based on ( $2^{-\Delta\Delta C_t}$ ). **(H)** Heatmap showing the relative expression of 11 selected transcripts from BM PBs and PCs from both WT and *Cxcr4*<sup>+/*1013*</sup> mice determined by Biomark multiplex qPCRs at day 6 post immunization. Data are presented by applying a column Z score based on ( $2^{-\Delta\Delta C_t}$ ). **(I)** Principal component analysis was performed on BM-PBs and BM-PCs from both groups using a correlation test. **(J)** Representative histograms for the indicated proteins from BM PBs and PCs from both WT and *Cxcr4*<sup>+/*1013*</sup> mice are shown. Results are from 2-3 independent experiments (Mean  $\pm$  SEM, n=4-10). Mann–Whitney U test was used to assess statistical significance (\*P $\leq$ 0.05, \*\* P<0.01, \*\*\*P<0.001).

**Figure 7: *Cxcr4* desensitization is essential to limit plasmablast maturation and persistence within the bone marrow:** **(A)** PB (B220<sup>lo</sup>CD138<sup>+</sup>) and PC (B220<sup>-</sup>CD138<sup>+</sup>) numbers in the BM of both WT or *Cxcr4*<sup>+/*1013*</sup> mice post NP-LPS immunization at the indicated time points. **(B)** Blimp1<sup>GFP/+</sup> PBs were generated *in vitro* from splenic B cells and labeled with CTV for *Cxcr4*<sup>+/*1013*</sup> cells and with CTY for WT cells as previously described in Fig 6D and transferred into WT recipient mice. Left: Representative dot plots of PC (Red) and PB (Blue) gating in the BM of recipient mice. Right: Total number of transferred Blimp1<sup>GFP/+</sup> PBs and

PCs in the BM of recipient mice at day 1 and 2 post transfer. **(C)** Left: Representative dot plots showing the frequency of CTV<sup>+</sup> (*Cxcr4*<sup>+/*1013*</sup> x Blimp1<sup>GFP/+</sup>) and CTY<sup>+</sup> (WT x Blimp1<sup>GFP/+</sup>) cells in both the PC (CD138<sup>+</sup>B220<sup>-</sup>) and PB (CD138<sup>+</sup>B220<sup>+</sup>) compartments in recipient mice at day 2 post transfer. Right: Quantification of the relative frequency of CTV<sup>+</sup> (*Cxcr4*<sup>+/*1013*</sup> x Blimp1<sup>GFP/+</sup>) and CTY<sup>+</sup> (WT x Blimp1<sup>GFP/+</sup>) in the PB and PC compartments of recipient mice at day 2 post transfer. **(D)** Heatmap showing the relative expression of B and PC master regulator genes presented as ( $2^{-\Delta\Delta Ct}$ ) in BM PCs and PBs from both genotypes at day 6 post NP-LPS immunization. Data are presented by applying a column Z score. **(E)** Number of total ASCs IgM<sup>+</sup> and NP15-IgM<sup>+</sup> in the BM assessed by ELIspot at the indicated time points post NP-LPS immunization. Results are from at least 2 representative experiments (**A-D** and **E**) or from two independent experiments (**C**) (Mean  $\pm$  SEM, n=2-9). Mann–Whitney U test was used to assess statistical significance (\*P<0.05, \*\* P<0.01, \*\*\*P<0.001).

Figure 1

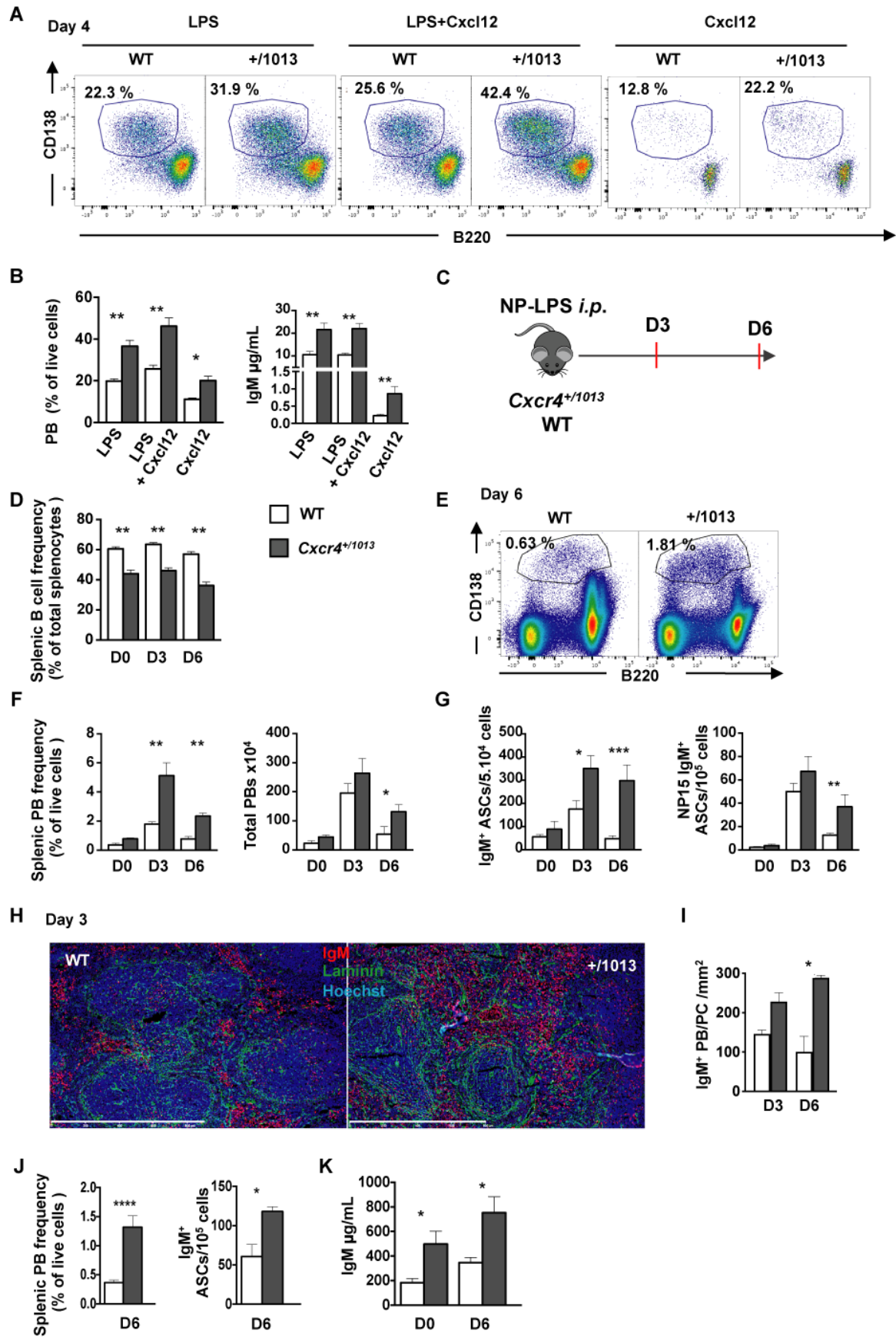


Figure 2

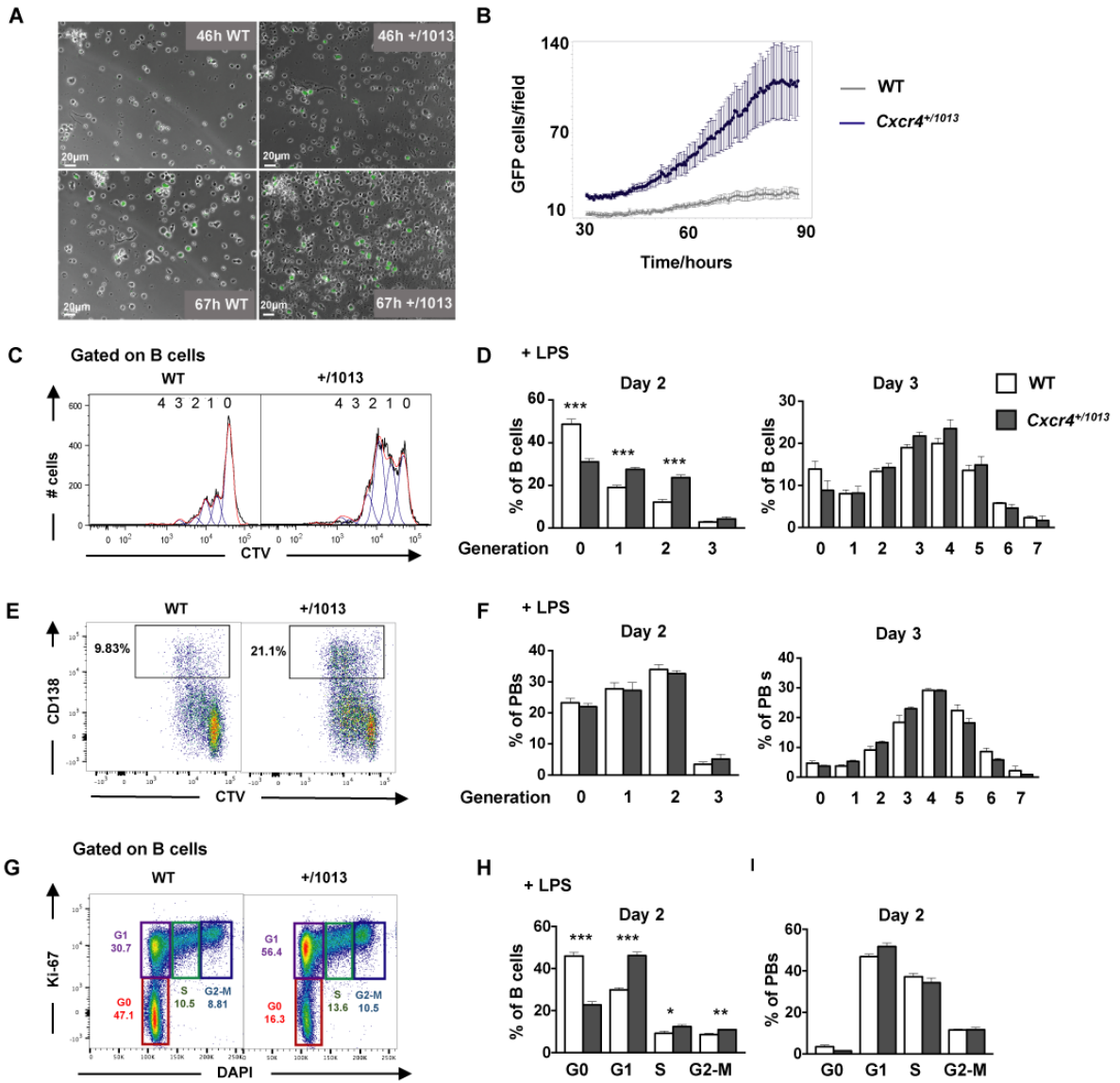


Figure 3

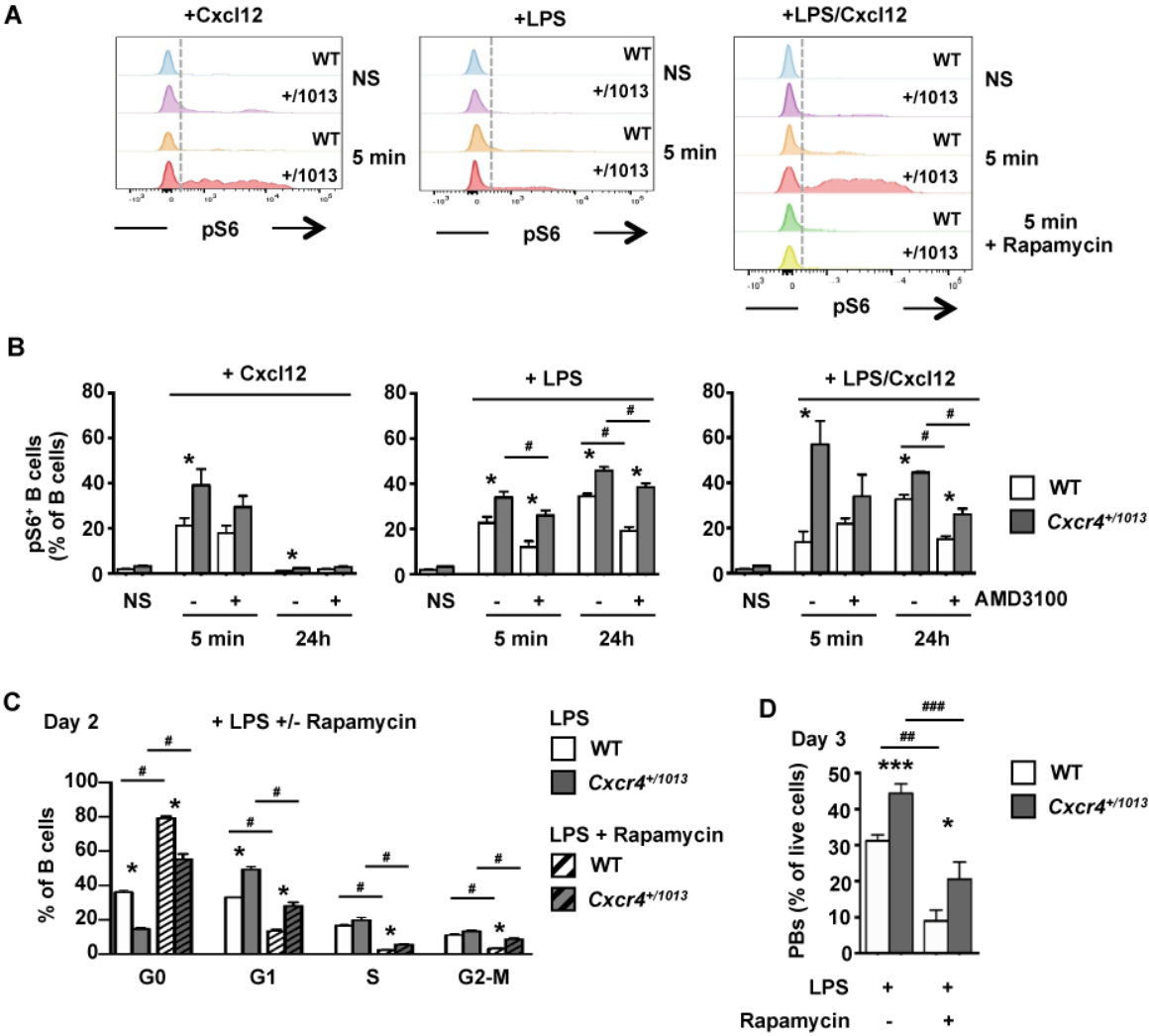


Figure 4

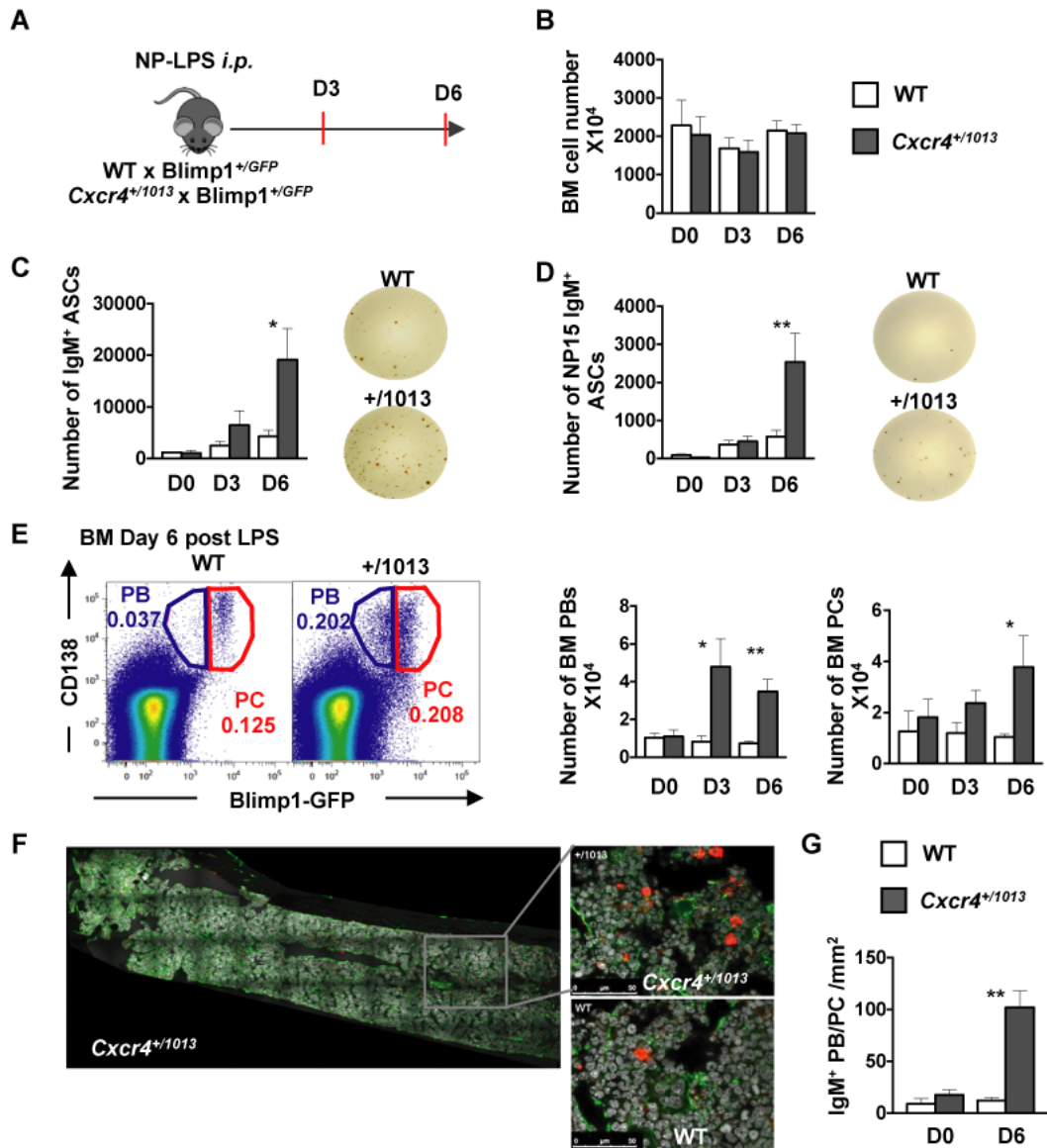


Figure 5

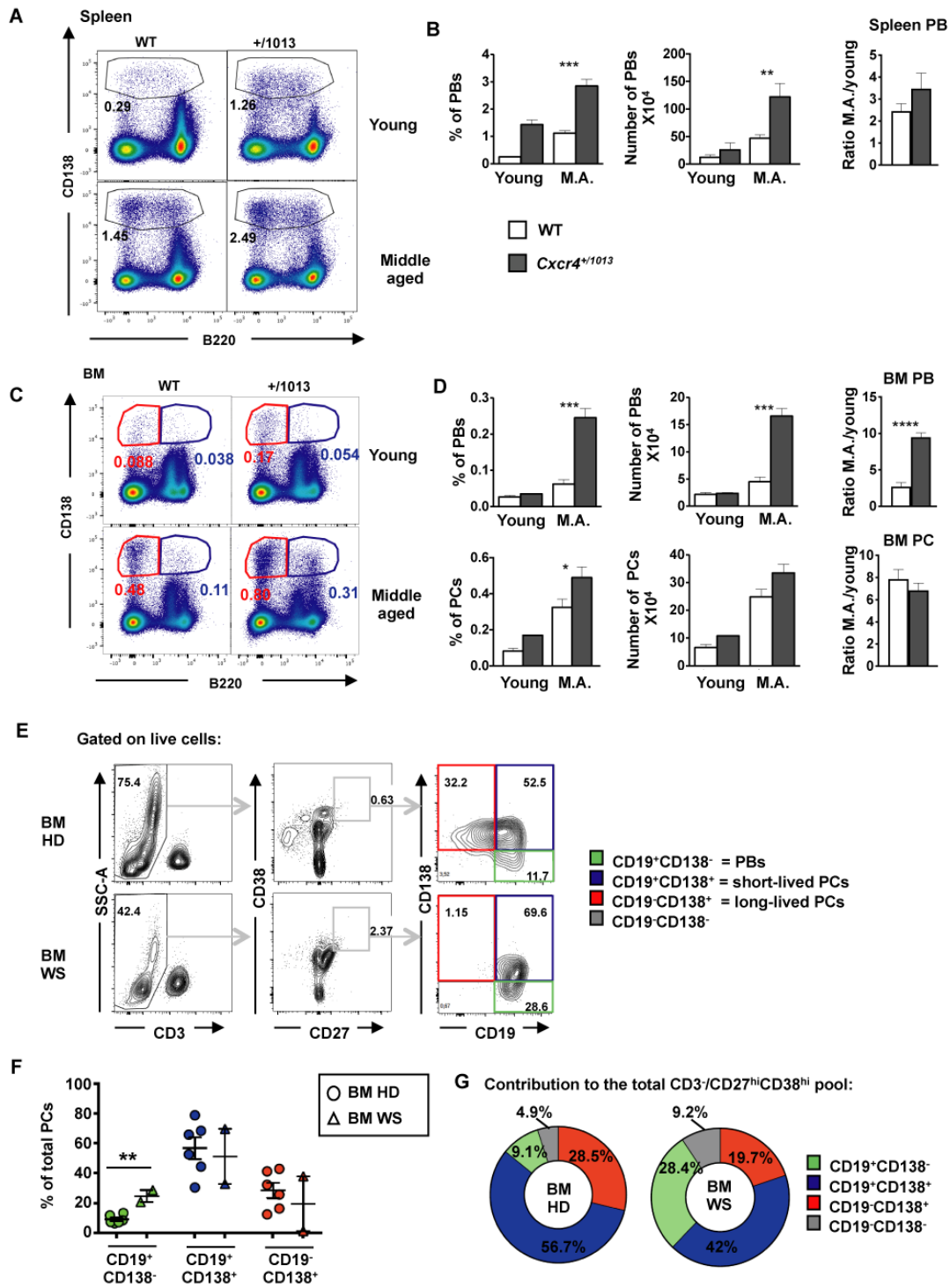


Figure 6

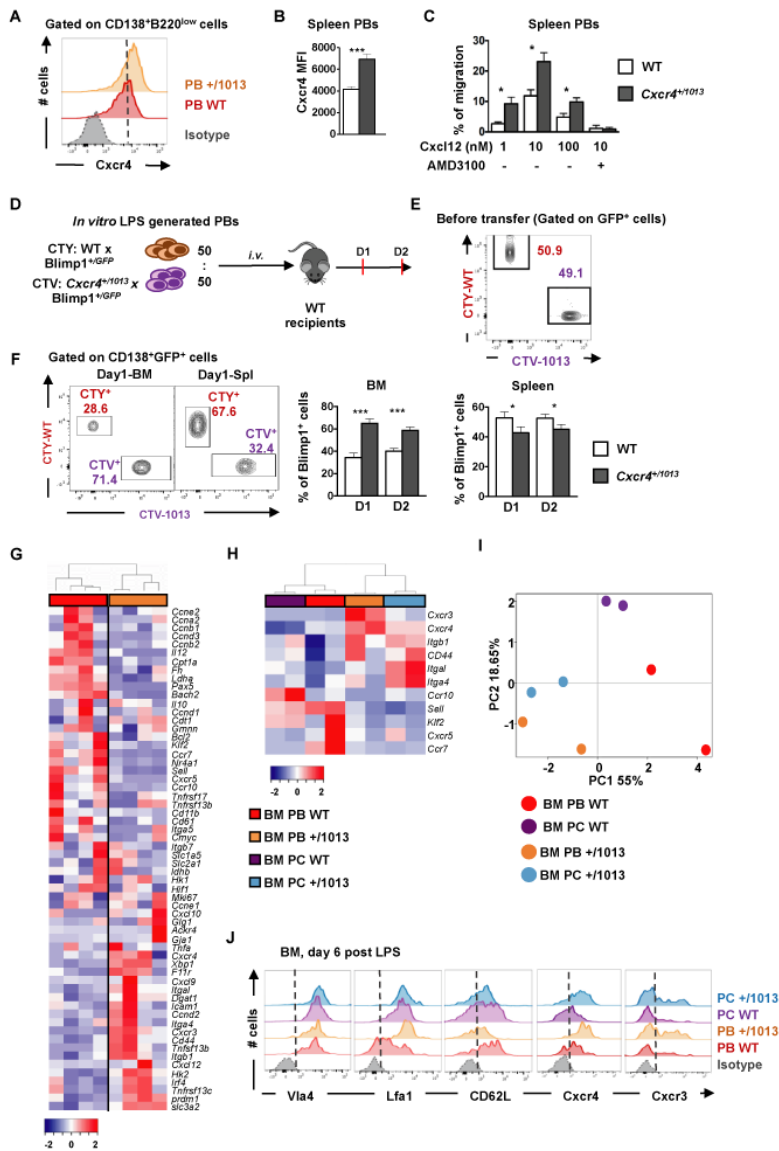


Figure 7

